Journal of Power Sources 395 (2018) 221–227

Contents lists available at ScienceDirect

Journal of Power Sources

journal homepage: www.elsevier.com/locate/jpowsour

Enhanced electricity generation and effective water filtration using graphene-based membrane air-cathodes in microbial fuel cells

Xiangru Song[a], Jia Liu[a,*], Qing Jiang[a], Youpeng Qu[b], Weihua He[a], Bruce E. Logan[c], Yujie Feng[a,*]

[a] State Key Laboratory of Urban Water Resource and Environment, Harbin Institute of Technology, No 73 Huanghe Road, Nangang District, Harbin 150090, China
[b] School of Life Science and Technology, Harbin Institute of Technology, No. 2 Yikuang Street, Nangang District, Harbin 150080, China
[c] Department of Civil and Environmental Engineering, Penn State University, 212 Sackett Building, University Park, PA, 16802, USA

HIGHLIGHTS

- Graphene was added to the activated carbon catalyst of an air cathode (AGM).
- The AGM air-cathode was made using a simple phase inversion method.
- Power and COD removal were improved in the MFC with AGM air-cathode.
- Anti-fouling properties of the AGM air-cathode were improved.

GRAPHICAL ABSTRACT

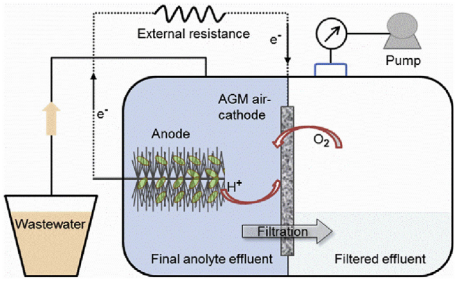

ARTICLE INFO

Keywords:
Microbial fuel cell
Graphene membrane air-cathode
Phase inversion method
Biofilm inhibition

ABSTRACT

Air-cathodes in microbial fuel cells that can also filter wastewater provide the dual benefits of electricity production and reduction of the effluent chemical oxygen demand. Air-cathodes prepared using a novel activated carbon/graphene membrane (2, 5 or 10% graphene by weight) prepared by phase inversion have good conductivities (5.6 ± 0.5 to 7.3 ± 0.6 mS cm^{-1}) compared to control (3.0 ± 0.4 mS cm^{-1}, activated carbon, no graphene). The cathode with 5 wt% graphene produces the highest maximum power density of 1460 ± 10 mW m^{-2}, which is 58% higher than that the control (928 ± 8 mW m^{-2}). The increased power is due to an 88% reduction in charge transfer resistance of 6.0 ± 0.3 Ω (cathode with 5 wt% graphene) compared to the control. Following a cycle of treatment and current generation, 60 ± 1% of the chemical oxygen demand is removed from the remaining chemical oxygen demand, producing an effluent chemical oxygen demand concentration of 20 ± 1 mg L^{-1}. Biomass (4.99 ± 0.02 mg-protein cm^{-2}) is decreased by 33% compared to the control. These results demonstrate that cathodes made with graphene can produce electricity and a high quality effluent with low cathode biofouling.

1. Introduction

Wastewater is a potential source, as it contains more energy than that needed to treat it using conventional wastewater treatment technologies [1,2]. While aerobic wastewater treatment technologies cannot be used to extract this energy, microbial fuel cells (MFCs) are bioelectrical technologies that can be used to harvest this energy and accomplish wastewater treatment [3–5]. For efficient power generation, air cathodes must be used in the MFCs to produce power as this avoids the need to aerate the water [6]. The oxygen reduction reaction (ORR) using an air-cathode MFC does not require water aeration, but the cathode needs to have excellent catalytic activity, a high oxygen

* Corresponding authors.
E-mail addresses: jia14921@163.com (J. Liu), yujief@hit.edu.cn (Y. Feng).

https://doi.org/10.1016/j.jpowsour.2018.05.043
Received 1 February 2018; Received in revised form 2 May 2018; Accepted 10 May 2018

transfer efficiency, and a high proton transfer to the catalyst site, and the cathode materials must be inexpensive and durable over time [7]. The most commonly used catalyst in MFCs is activated carbon, as it is inexpensive and it resists fouling better than platinum over long term operation [8]. However, the cathode can limit power generation in MFCs, and thus it is important to improve the ORR to increase power production.

Graphene is a pure carbon material which can be formed as an atom-thick sheet [9] or used with many layers as a dense honeycomb crystal structure [10–12]. Graphene has several features which are all useful characteristics for the ORR in MFC cathodes, including high electron transfer rates, a large specific surface area, excellent electrical conductivity and electrochemical stability, and good mechanical flexibility [13]. Recent research has shown that graphene can be added to an MFC cathode to improve performance and power densities of MFCs [14]. The three-dimensional structure of the graphene improved the ORR, which increased power production compared to plain activated carbon cathodes [15]. Nitrogen-doped graphene can have even better performance than plain graphene, as it has been shown to compare well to a Pt/C control in terms of polarization data and number of electrons transferred [16]. However, cathodes previously made using activated carbon and graphene have only been made using a traditional multiple-step, and energy-intensive press method.

A phase inversion process was recently used as a novel one-step approach to produce both the catalytic and diffusion layers of an air-cathode [17]. This method was shown to be very simple, and making cathodes using this method significantly reduced the total cost of the MFC [18]. The phase inversion process used hydrophobic polyvinylidene fluoride (PVDF) to bind the activated carbon catalyst to a stainless steel mesh current collector [17,19,20]. It was further demonstrated that water retention could be increases using an additional PVDF membrane on the air-facing side of the cathode [17]. However, for some MFC applications the cathode has been designed to allow water filtration, thus accomplishing both power generation and filtration of the effluent [21]. In this case, the choice of the binder is essential to allow water passage rather than water retention. Polyvinyl chloride (PVC) is a polymer that can be used to produce low-cost porous and ultrafiltration membranes that have a good water fluxes and particle rejection properties [22,23].

The key performance data for the MFC were power generation and effluent quality [24]. In order to produce an MFC with good performance and a cathode with effective water filtration, an activated carbon/graphene membrane air-cathode (AGM air-cathode) was developed here. It was manufactured by a phase inversion process. The charge transfer, filtration, and antifouling properties were the key parameters in evaluating the performance of the membrane cathodes [25]. The AGM air-cathode possessed improved electrochemical performance and antifouling properties compared to a plain activated carbon membrane, and it was easily produced by the phase inversion process.

2. Material and methods

2.1. Materials

PVC (80,000 g mol^{-1}) was provided by Shenyang Chemical Co., LTD. N,N-dimethylacetamide (DMAc, anhydrous, 99.8%) was purchased from Tianjin Fuyu Fine Chemical Co., Ltd (Tianjin, China) and 1-methyl-2-pyrrolidinone (NMP, AR) was obtained by Tianjin Zhiyuan Chemical Reagent Co., Ltd (Tianjin, China). Polyvinylpyrrolidone (PVP, k30, AR) was obtained from Tianjin Guangfu Fine Chemical Research Institute (Tianjin, China) and used as a pore-forming agent. Polyaniline (PANI, 300 kDa, Hubei Yuanchengsaichuang Co., Ltd, Wuhan, China) was used to promote oxygen adsorption and electrode conductivity [26]. Activated carbon powder (AC, Carbosino Material Co., Ltd, Shanghai, China) as the electrode substrate, and graphene (G, Suzhou Hengqiu Co., Ltd, Suzhou, China) as a modifier, were used in the preparation of an electrically conductive membrane.

2.2. Membrane air-cathode preparation

The PVC binder and PVP pore-forming agent (PVC-co-PVP; 12 wt% PVC and 6 wt% PVP) were dissolved in DMAc at ambient temperature in the dark, and mixed using a stir bar for over 24 h to allow them to completely dissolve. The polymer was then placed in the dark for an additional 24 h to allow removal of gas bubbles. PVC-co-PVP (0.81 g), activated carbon (0.58 g), and PANI (0.15 g) were mixed with NMP (3 mL). Graphene (G, Suzhou Hengqiu Co., Ltd, Suzhou, China) was then added into the carbon powder at four different mass ratios (G:AC) of 0 (denoted as control), 0.02 (G2), 0.05 (G5) and 0.10 (G10). After sonicating of the mixture for 30 min at ambient temperature, the homogenized solution was coated onto both two sides of a stainless steel mesh, and then immersed into a coagulation bath (deionized water at ambient temperature) for 20 min to complete coagulation.

2.3. Structure and membrane properties

The morphologies of the membrane air-cathode were observed using a scanning electron microscope (SEM, Hitachi Ltd. S-4700) [27]. Atomic force microscopy (AFM, Veeco Instruments Inc, USA) was used to characterize the roughness of the membrane air-cathode, with the images analyzed using the Nanoscope III software [28]. Contact angles were measured using a sessile drop technique and a surface contact angle measurement instrument (the type JYSP-360, USA, needlepoint 1.5 mm) [29]. The contact angle was tested after water droplets stabilized for 20 s. The surface energies (γ_{SV}, mN m^{-1}) were calculated as: $\gamma_{SV} = \gamma_{SV}^{P} + \gamma_{SV}^{D}$ and $\gamma_{LV}(1 + cos\theta) = 2\sqrt{\gamma_{SV}^{D}\gamma_{LV}^{D}} + 2\sqrt{\gamma_{SV}^{P}\gamma_{LV}^{P}}$ using the experimentally determined intrinsic contact angles of water (γ_{LV} = 72.8 mN m^{-1}, γ_{LV}^{D} = 21.8 mN m^{-1}, γ_{LV}^{P} = 51.0 mN m^{-1}) and methylene iodide (γ_{LV} = 58.2 mN m^{-1}, γ_{LV}^{D} = 39.5 mN m^{-1}, γ_{LV}^{P} = 18.7 mN m^{-1}) [30]. The membrane conductivities were tested using a digital four – probe tester (ST2263, Suzhou Jingge Electronic Co., Ltd, China). Porosity was measured by a gravimetric method as $\varepsilon = (W_w - W_d)/AH\rho_w$, where W_w is the wet weight (g), W_d is the dry weight (g), L is the membrane thickness (cm), A is the exposed membrane area (cm^2), and ρ_w is the density of water (g cm^{-3}) [31]. The cathode wet weight, W_w, was measured after wiping excessive water on the cathode surfaces with filter paper. The dry weight, W_d, was measured after drying the cathodes in oven at 50 °C for 48 h. The pure water flux ($L_P = V/\Delta PAt$) (L_P, L m^{-2} s^{-1} MPa^{-1}) was calculated as previously described, where V (L) is the volume, ΔP (MPa) is the pressure, and t (s) is the time [32]. The flux attenuation (J_w, %) was characterized the antifouling performance of the membrane cathode, which was calculated by $J_w = (J_0 - J_t)/J_0 \times 100\%$, where J_0 (L m^{-2} s^{-1} MPa^{-1}) is the initial flux, and J_t (L m^{-2} s^{-1} MPa^{-1}) is the stable operating flux [33].

2.4. Electrochemical characterization

All electrochemical measurements of the membrane air-cathode were performed with an electrochemical workstation (Auto Lab PGSTAT128 N, Metrohm, Swiss) in a single cell with a three-electrode system, consisting of a membrane air-cathode as the working electrode, a saturated calomel electrode as the reference electrode (+242 mV vs. SHE, Spsic-Rex Instrument Factory, China), and a Pt sheet (1 cm^2) as the counter electrode. The electrolyte for all tests was a 50 mmol L^{-1} phosphate buffer solution (conductivity of 6.9 mS cm^{-1}) at ambient temperature (25 °C). Linear sweep voltammetry (LSV) was conducted over a potential range of −0.3 V to 0.3 V, at a scan rate 1 mV s^{-1} [34]. Electrochemical impedance spectroscopy (EIS) tests were performed at a frequency range of 10 mHz–100 kHz with amplitude of 5 mV [35].

2.5. MFC construction and operation

The single chamber, air-cathode cubic MFC reactor was constructed as previously described, with a total liquid volume of 28 mL [36]. Graphite fiber brush anodes (3 cm in length and 3 cm in diameter) were heat-treated at 450 °C for 30 min [37].

During start-up, MFCs were inoculated with 30% domestic wastewater collected from a municipal sewer (Harbin, China) and 70% sodium acetate (1 g L^{-1}). After a reproducible cycle of voltage was produced, the MFCs were operated using sodium acetate (1 g L^{-1}) in a phosphate buffer solution (PBS, 50 mM) containing: NH_4Cl (0.31 g L^{-1}); $NaH_2PO_4{\cdot}2H_2O$ (3.32 g L^{-1}); $Na_2HPO_4{\cdot}12H_2O$ (10.32 g L^{-1}); KCl (0.13 g L^{-1}), a metal (12.5 mL) and vitamin (12.5 mL) solution [38,39]. All test conditions were conducted using duplicate reactors in a constant temperature room (30 °C). The voltage of MFC device across an external resister (1000 Ω, except during polarization tests) was monitored using a precision data acquisition system.

2.6. Power generation and COD removal

Polarization tests were obtained by varying external resistance from open circuit potential to 50 Ω. The power and current densities were normalized by the projected cathode surface area. The power density (P, mW m^{-2}) was calculated as $P = U^2/RA$, where U (V) is the cell voltage, R (Ω) is the external resistance [40]. The current density (I, A m^{-2}) was obtained from $I = U/RA$ [41]. Power density and polarization data were obtained after the reactors were considered to have reached steady state based on repeatable peak potentials for three consecutive batch cycles.

Chemical oxygen demand (COD) measurements were measured using standard methods with HACH DR/3900 Spectrophotometer (HACH Co., Loveland, Co., USA) [42]. The tCOD was obtained directly from the anode chamber (final anolyte tCOD, $tCOD_f$, mg L^{-1}) and air chamber (filtered effluent tCOD, $tCOD_{eff}$, mg L^{-1}) (Fig. S1). The rejection COD ($tCOD_r$, mg L^{-1}) was calculated by $tCOD_r = tCOD_f - tCOD_{eff}$. The rejection percentage (J_{tCOD}, %) of membrane air-cathode to tCOD was obtained with $J_{tCOD} = tCOD_r/tCOD_f \times 100\%$.

2.7. Cathode biofouling

In order to evaluate fouling of the membrane air-cathode, the mass of biofilm on the cathode surface was evaluated in terms of its protein content after 3 months of operation in fed-batch mode, without any cathode cleaning. Biofilm was removed from the liquid-side surface of the cathode using a knife, and the sample was placed in a centrifuge tube with 10 mL of 0.2 N NaOH for 1 h (4 °C), and then mixed the solution using a vortex mixer (XK96–A, Xinkang Medical Instrument Co., Ltd, China) every 15 min for 10 s to fully extract the protein. The extracted liquid was transferred using a pipette into a new centrifuge tube. After rinsing the residue with 10 mL of deionized water, the liquid was mixed with extracted liquid to obtain 20 mL of 0.1 N NaOH. The obtained liquid was frozen at −20 °C for 2 h and then thawed at 90 °C for 10 min, and this freeze-thaw cycle repeated three times. Finally, the protein content of the obtained liquid was measured using a commercial kit using the bicinchoninic acid (BCA) method [43] (Sangon Biotech Co., Ltd (Shanghai, China).

3. Results and discussion

3.1. Morphology of the membrane air-cathode

SEMs of the membrane air-cathodes (Fig. 1) showed that increasing the content of graphene in the casting solution was beneficial to the serrated aperture formation, which was likely due to differences in the formation and separation speed of the pore-forming agent from the polymers and graphene. The surface of unmodified membrane air-cathode (denoted as the control) had a compact texture with little porosity. The size of the pores was gradually increased with graphene addition. The maximum porosity of 77 ± 1% was obtained for G5, which was 64% higher than that of control (47 ± 1%) (Fig. S2). When the content of graphene was further increased to G10, the porosity slightly decreased to 71 ± 1%.

AFM images of the membrane air-cathodes also showed differences in morphologies before and after graphene addition (Fig. 2). The three-dimensional images clearly showed that the surface roughness of the membrane air-cathodes was decreased after addition of graphene (Fig. S3). The average roughness was decreased by 61% from 88 ± 6 nm (control) to 34 ± 2 nm (G5). The roughness of G2 (47 ± 7 nm) and G10 (43 ± 7 nm) were similar to each other, and intermediate relative to these other samples. Thus adding graphene decreased the surface roughness of the electrodes, which is beneficial for making them more resistant to biofouling, as shown in other membrane studies that biofouling is increased for rougher surface [44].

3.2. Membrane characteristics of the membrane air-cathode

In order to determine changes in the membrane air-cathode hydrophobicity, contact angle measurements were performed on all cathodes. The electrodes modified by graphene had lower contact angles than the control, with the contact angles decreasing by 30% from 104.2 ± 0.5° (control) to 73.1 ± 0.6° (G10) (Fig. 3A). This reduction indicated that the surfaces of the membrane air-cathode modified by graphene addition become more hydrophilic, which would enhance its resistance to biofilm formation and improve water permeability [45].

Surface energies were significantly increased by adding graphene, and they increased in proportion to the amount of graphene used in the cathode. The maximum surface energy of 43.3 ± 0.2 mN m^{-1} was obtained with G10, which was 135% higher than the control (18.4 ± 0.2 mN m^{-1}). This surface energy for G10 was also 5% higher than G5 (41.3 ± 0.8 mN m^{-1}) and 34% higher than G2 (32.3 ± 0.1 mN m^{-1}). Higher surface energies should lead to less biofouling [46].

The water flux of the membrane air-cathode increased with the addition of graphene (Fig. 3B). Water flux of the control electrode (20 ± 1 L $m^{-2}s^{-1}$ MPa^{-1}) was increased by 25% to a maximum of 25 ± 1 L $m^{-2}s^{-1}$ MPa^{-1} for G10. The improvement of the water flux of membrane air-cathode was consistent with SEM measurements showing larger porosities of the cathodes with increased content of graphene.

The conductivities of the cathodes, evaluated using a four-probe measurement (Fig. S4), showed that the G5 cathode had the maximum electrical conductivity of 7.3 ± 0.6 mS cm^{-1}, which was 1.4 times higher than the control (3.0 ± 0.4 mS cm^{-1}). This was also 14% higher than the G2 cathode (6.4 ± 0.3 mS cm^{-1}) and 30% higher than the G10 cathode (5.6 ± 0.5 mS cm^{-1}). The conductivity of G10 was lower than that of G5, which may be because of the reuniting of graphene. With a low graphene loading, the graphene sheets could be distributed more homogeneously as a 3D conductive network, creating an abundance of transfer channels in the cathode. In the membrane cathode with a high graphene loading, the graphene sheets could have overlapped with each other, which would have led to more of a blocking effect, and lessened electron transmission [47,48].

3.3. Electrochemical analysis of the membrane air-cathode

The current densities of all of the AGM air-cathodes were higher than that of the control cathode based on an LSV analysis (Fig. 4A). For example, at a potential of −0.1 V (vs. SCE), the G5 cathode had the highest current density of 8.0 mA cm^{-2}, which was 58% higher than the control (5.2 mA cm^{-2}), with lower current densities obtained for the G2 (7.0 mA cm^{-2}) and G10 (6.5 mA cm^{-2}) cathodes.

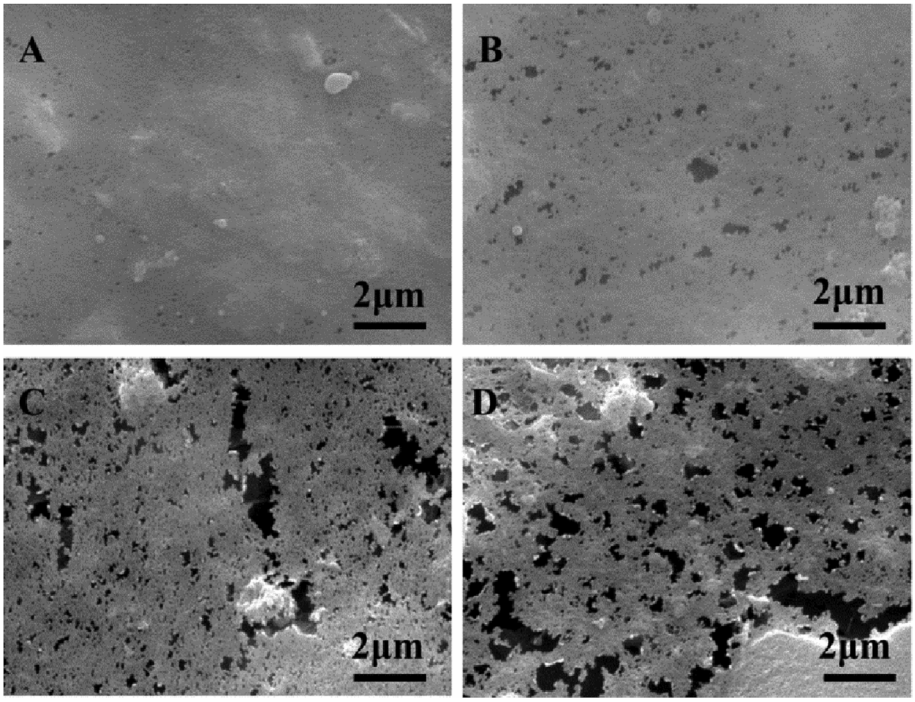

Fig. 1. SEM surface images (magnification = ×10,000, scale bar = 2 μm) of the AGM and control air-cathodes. (A) control (no graphene), (B) G2, (C) G5 and (D) G10.

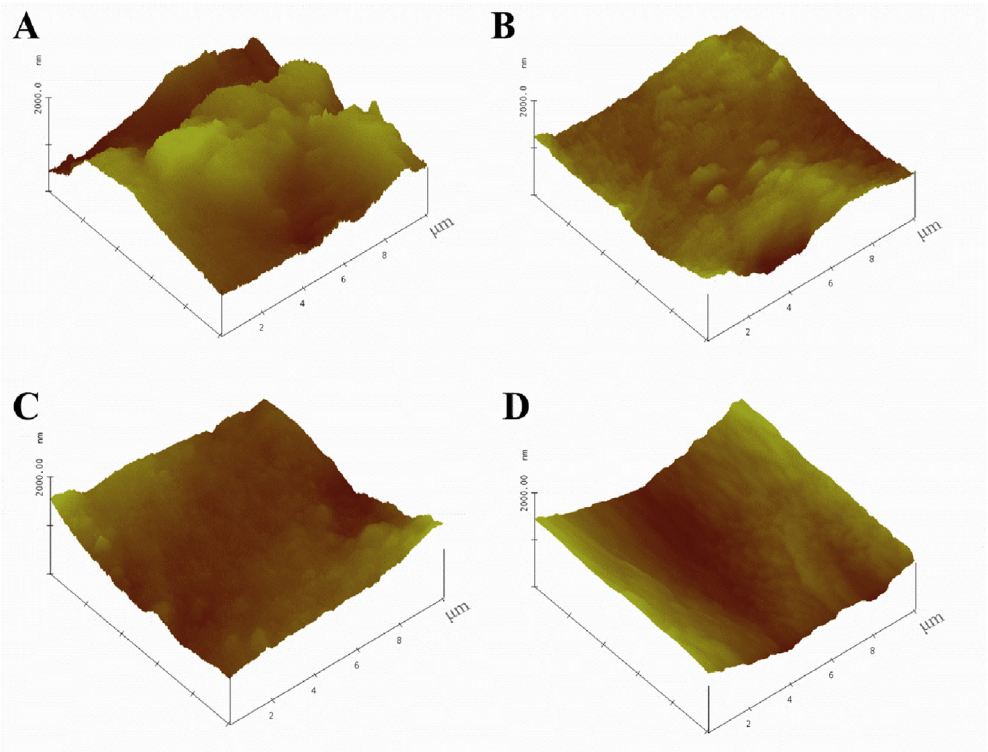

Fig. 2. Three dimensional AFM images of the AGM and control air-cathodes at a scan size of 10 μm × 10 μm: (A) control, (B) G2, (C) G5 and (D) G10.

The G5 cathode exhibited the lowest charge transfer resistance (R_{ct}) of 6.0 ± 0.3 Ω, which was reduced by 88% compared with control (50.0 ± 1.3 Ω), and 49% lower than the G10 (11.7 ± 0.9 Ω) (Fig. 4B). The R_{ct} of G2 (6.4 ± 0.1 Ω) was slightly lower than that of G5. The significant decrease in R_{ct} reflected the improved charge transfer with graphene addition due to its two-dimensional structure of graphene [49].

The exchange current density (i_0) of the electrodes was calculated as shown by the Tafel plot (Fig. 5). The maximum exchange current density of 1.30×10^{-4} A cm^{-2} was obtained using G5, which was 79% higher than that of control (7.28×10^{-5} A cm^{-2}), 12% higher than G2 (1.15×10^{-4} A cm^{-2}) and 17% higher than G10 (1.11×10^{-4} A cm^{-2}). These LSV, EIS and Tafel analysis results demonstrated that adding graphene significantly improved the catalytic

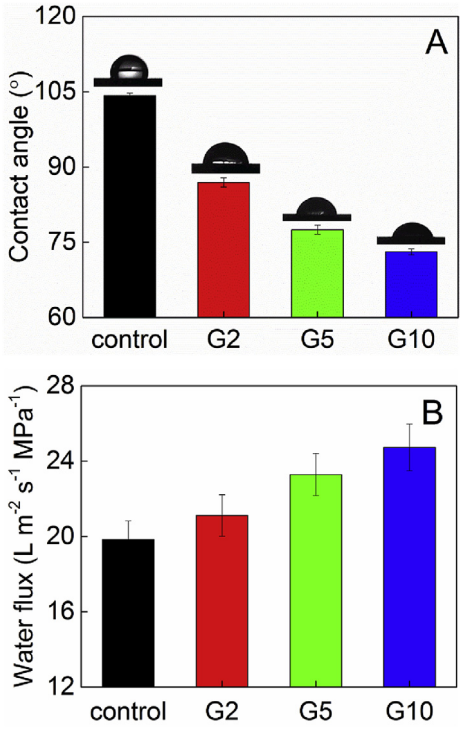

Fig. 3. (A) Surface contact angle and (B) Water flux of the AGM and control air-cathodes The contact angles were obtained after stabilizing of water drop 20 s. Error bars ± SD were based on averages measured in triplicate.

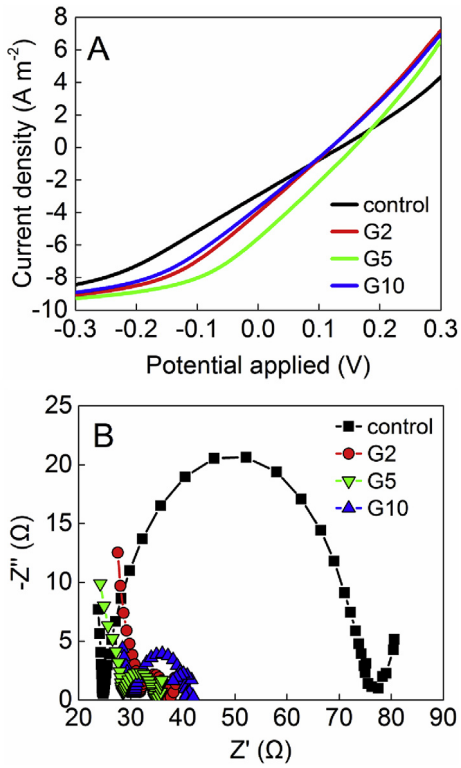

Fig. 4. (A) LSV curves and (B) Nyquist plots of the AGM and control air-cathodes in 50 mM PBS.

activities of the cathodes, likely by a combination of the increased electrical conductivities due to the graphene [50] and the improved hydrophilicity [51].

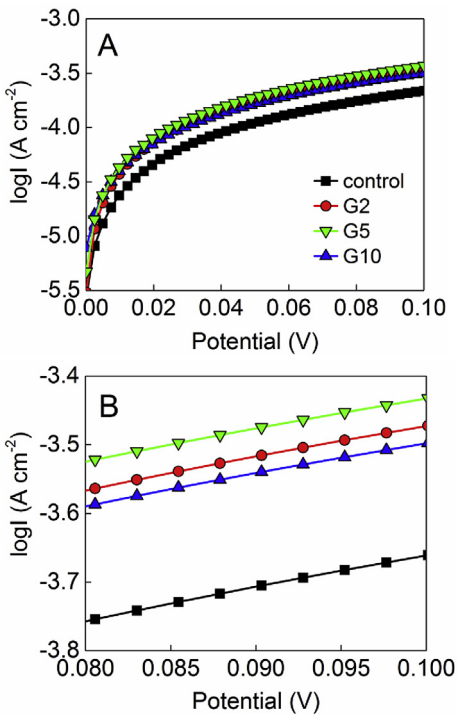

Fig. 5. (A) Tafel curves and (B) fitted curves of the AGM and control air-cathodes from 0.08 V to 0.1 V.

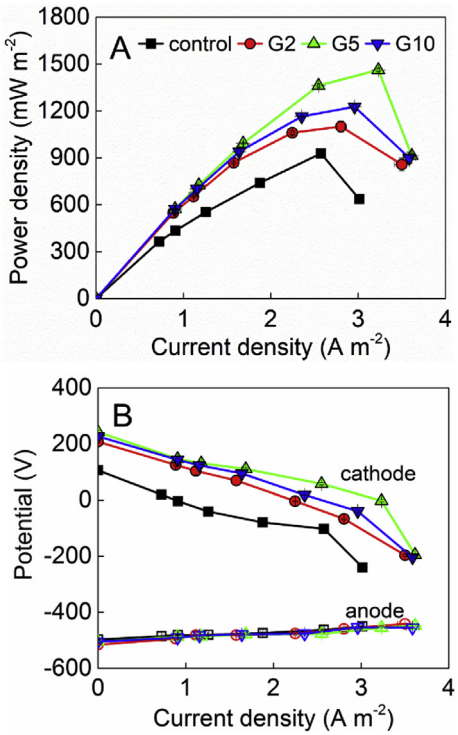

Fig. 6. (A) Power density curves and (B) potential curves for the AGM and control air-cathodes.

3.4. MFC performance

Power densities of MFCs with the G2, G5 and G10 cathodes were all higher than the control (928 ± 8 mW m^{-2}) (Fig. 6). The maximum power density was 1460 ± 10 mW m^{-2} for G5 membrane air-cathode, which was 58% higher than the control (Figs. 6A), 19% higher than that

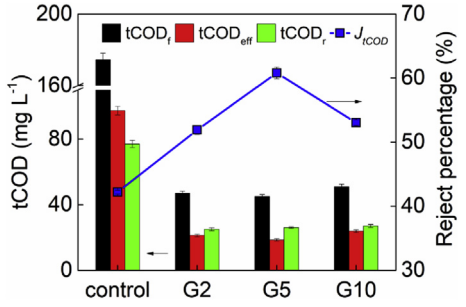

Fig. 7. Effluent COD concentrations and reject percentage for the AGM and control air-cathodes ($tCOD_f$ was final anolyte effluent tCOD, $tCOD_{eff}$ was filtrated effluent tCOD by the air-cathode, $tCOD_r$ was rejected COD by the air-cathode, J_{tCOD} was rejection percentage to tCOD).

of G10 (1230 ± 20 mW m^{-2}), and 33% higher than that of G2 (1100 ± 40 mW m^{-2}). The increased power production was clearly due to the improved performance of the cathodes, as the anode potential curves were all nearly identical (Fig. 6B). The cathodes possessed higher conductivity and lower charge transfer resistance after adding of graphene, which could enhance the electron transfer and benefit power generation [49].

The final anolyte and filtered effluent COD concentrations with the G2, G5 or G10 cathodes were all lower than the control ($tCOD_f$ = 175 ± 4 mg L^{-1}, $tCOD_{eff}$ = 98 ± 3 mg L^{-1}) (Fig. 7). The lowest final anolyte tCOD was 45 ± 1 mg L^{-1} for G5 cathode, which was reduced by 74% compared with control. The lowest filtered effluent COD was $tCOD_{eff}$ = 19 ± 1 mg L^{-1} for G5 cathode, which was 81% lower than the control, 21% lower than the G10 ($tCOD_{eff}$ = 24 ± 1 mg L^{-1}), and 10% lower than the G2 ($tCOD_{eff}$ = 21 ± 1 mg L^{-1}). The rejection percentage to tCOD of G2, G5, and G10 were all higher than the control (42 ± 1%). The maximal rejection percentage to tCOD was 60 ± 1% for G5, which was increased by 43% compared with control, 15% higher than the G2 (52 ± 1%), and 13% higher than the G10 (53 ± 1%). These results showed that the AGM air-cathodes improved the COD removal in the MFC.

3.5. Membrane antifouling performances

The flux attenuation percentage of G2, G5 and G10 were all lower than the control (13.2 ± 0.7%) (Fig. 8A), showing that adding graphene reduced biofouling. The minimal flux attenuation percentage was 5.4 ± 0.2% for G10, which was 59% less than the control, and 23% lower than G2 (7.0 ± 0.3%). The flux attenuation percentage of G5 was 5.7 ± 0.1%, which was 57% lower than the control.

Biofilm accumulation was reduced with graphene addition. The highest protein content of 7.43 ± 0.02 mg-protein cm^{-2} was produced by the control (Fig. 8B). The lowest protein concentration was 4.99 ± 0.02 mg-protein cm^{-2} for G10, which was 33% less than the control, and 14% lower than G2 (5.78 ± 0.02 mg-protein cm^{-2}). The protein content of G5 was 5.31 ± 0.02 mg-protein cm^{-2}, which was 29% lower than the control. These flux attenuation and biofilm accumulation results indicated that adding graphene enhanced the biofouling resistance of the air-cathodes. The antifouling performance was consistent with the hydrophilicity and surface roughness. The membrane cathode after loading graphene had a lower surface roughness than that of the control. The modified cathode had a smoother surface which would have improved its antifouling ability [52]. The hydrophilicity of membrane cathode was increased by graphene, which decreased the surface adsorption and reduced membrane fouling [53].

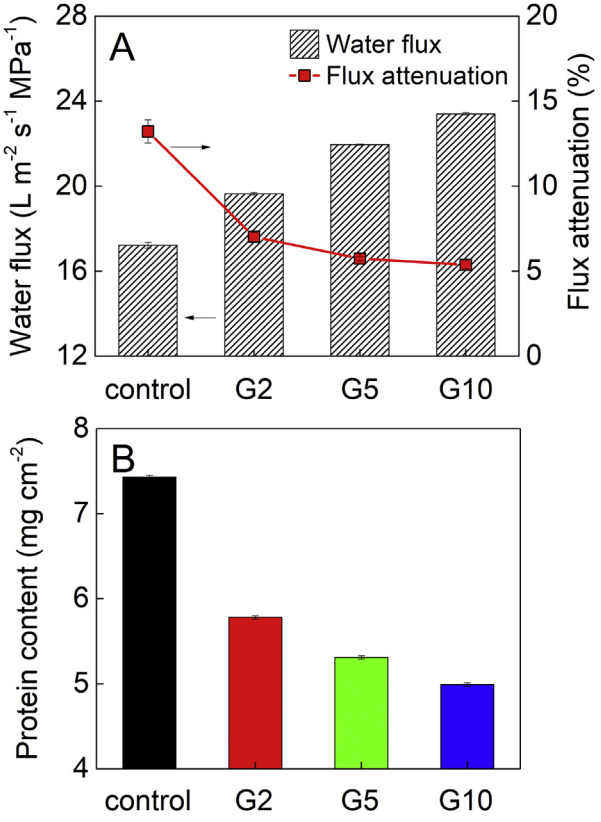

Fig. 8. (A) Water flux and flux attenuation, (B) Protein content of the AGM and control air-cathodes. Error bars ± SD were based on averages measured in triplicate.

4. Conclusions

The membrane air-cathode containing graphene was fabricated using a phase inversion method to enhance the performance of MFC and provide a filtered effluent. The addition of graphene resulted in multiple improvements in operation, including increased electricity generation, improved filtration which resulted in a lower effluent COD, and antifouling characteristics as demonstrated by less biofilm formation on the cathode. The optimal condition was obtained by using the G5 cathode (5% graphene), which increased the power density by 58% compared to the control reactor. Increases in the cathode hydrophilicity and the water flux demonstrated that graphene addition significantly affected the three-phase interface and properties of the membrane. The enhanced COD removal rate and reduced biofilm formation (decreased by 33%) demonstrated the improved wastewater processing efficiency using the MFC. These results showed that a graphene modified membrane prepared by the phase inversion method was a simple and effective method for improving air-cathode performance in an MFC.

Acknowledgments

This work was supported by the National Key R&D Program of China (Grant No. 2016YFE0106500), National Natural Science Fund of China (Grant No. 51408156), and Open Project of State Key Laboratory of Urban Water Resource and Environment, Harbin Institute of Technology (No. QA201609-01). Authors also acknowledged the International Cooperating Project between China and European Union (Grant No. 2014DFE90110).

Appendix A. Supplementary data

Supplementary data related to this article can be found at http://dx.

doi.org/10.1016/j.jpowsour.2018.05.043.

References

[1] P.L. McCarty, J. Bae, J. Kim, Environ. Sci. Technol. 45 (2011) 7100–7106.
[2] H.Y. Yuan, Z. He, Nanoscale 7 (2015) 7022–7029.
[3] D. Pant, A. Singh, G. Van Bogaert, S.I. Olsen, P.S. Nigam, L. Diels, K. Vanbroekhoven, RSC Adv. 2 (2012) 1248–1263.
[4] Y. Qiao, S.J. Bao, C.M. Li, Energy Environ. Sci. 3 (2010) 544–553.
[5] C.H. Feng, F.B. Li, H.Y. Liu, X.M. Lang, S.S. Fan, Electrochim. Acta 55 (2010) 2048–2054.
[6] F. Zhang, S.A. Cheng, D. Pant, G. Van Bogaert, B.E. Logan, Electrochem. Commun. 11 (2009) 2177–2179.
[7] Q. Wen, S.Y. Wang, J. Yan, L.J. Cong, Y. Chen, H.Y. Xi, Bioelectrochemistry 95 (2014) 23–28.
[8] E. Martin, B. Tartakovsky, O. Savadogo, Electrochim. Acta 58 (2011) 58–66.
[9] K.S. Novoselov, A.K. Geim, S.V. Morozov, D. Jiang, Y. Zhang, S.V. Dubonos, I.V. Grigorieva, A.A. Firsov, Science 306 (2004) 666–669.
[10] A.K. Geim, K.S. Novoselov, Nat. Mater. 6 (2007) 183–191.
[11] A.K. Geim, Science 324 (2009) 1530–1534.
[12] M.D. Stoller, S.J. Park, Y.W. Zhu, J.H. An, R.S. Ruoff, Nano Lett. 8 (2008) 3498–3502.
[13] Y.C. Yong, X.C. Dong, M.B. Chan-Park, H. Song, P. Chen, ACS Nano 6 (2012) 2394–2400.
[14] H.Y. Wang, G.M. Wang, Y.C. Ling, F. Qian, Y. Song, X.H. Lu, S.W. Chen, Y.X. Tong, Y. Li, Nanoscale 5 (2013) 10283–10290.
[15] C. Santoro, M. Kodali, S. Kabir, F. Soavi, A. Serov, P. Atanassov, J. Power Sources 356 (2017) 371–380.
[16] Y. Liu, H. Liu, C. Wang, S.X. Hou, N.A. Yang, Environ. Sci. Technol. 47 (2013) 13889–13895.
[17] W.L. Yang, W.H. He, F. Zhang, M.A. Hickner, B.E. Logan, Environ. Sci. Technol. Lett. 1 (2014) 416–420.
[18] C. Jin, C.H. Yang, F.L. Chen, Ecs Transactions, 35 2011, pp. 2987–2995.
[19] W.L. Yang, K.Y. Kim, B.E. Logan, Bioresour. Technol. 197 (2015) 318–322.
[20] W.L. Yang, F. Zhang, W.H. He, J. Liu, M.A. Hickner, B.E. Logan, J. Power Sources 269 (2014) 379–384.
[21] L. Malaeb, K.P. Katuri, B.E. Logan, H. Maab, S.P. Nunes, P.E. Saikaly, Environ. Sci. Technol. 47 (2013) 11821–11828.
[22] S. Mei, C.F. Xiao, X.Y. Hu, J. Appl. Polym. Sci. 120 (2011) 557–562.
[23] H. Rabiee, V. Vatanpour, M.H.D.A. Farahani, H. Zarrabi, Separ. Purif. Technol. 156 (2015) 299–310.
[24] R. Nitisoravut, C.N.D. Thanh, R. Regmi, Int. J. Green Energy 14 (2017) 712–723.
[25] L. Xu, Y.Q. Zhao, L. Doherty, Y.S. Hu, X.D. Hao, Crit. Rev. Environ. Sci. Technol. 46 (2016) 60–91.
[26] J. Kankare, I.A. Vinokurov, Anal. Chem. 69 (1997) 2337–2342.
[27] J. Liu, Y.J. Feng, X. Wang, X.X. Shi, Q. Yang, H. Lee, Z.H. Zhang, N.Q. Ren, J. Power Sources 196 (2011) 8409–8412.
[28] J. Liu, J.F. Liu, W.H. He, Y.P. Qu, N.Q. Ren, Y.J. Feng, J. Power Sources 265 (2014) 391–396.
[29] Q. Du, J.K. An, J.H. Li, L.A. Zhou, N. Li, X. Wang, J. Power Sources 343 (2017) 477–482.
[30] C. Boo, J. Lee, M. Elimelech, Environ. Sci. Technol. 50 (2016) 8112–8119.
[31] Q.Y. Zhang, C.D. Vecitis, J. Membrane Sci. 459 (2014) 143–156.
[32] L.H. Huang, X.F. Li, Y.P. Ren, X.H. Wang, RSC Adv. 7 (2017) 20824–20832.
[33] Q.H. Zhou, Z. Wang, H.J. Shen, Z.Y. Zhu, L.P. Liu, L.B. Yang, L.N. Cheng, J. Chem. Technol. Biotechnol. 91 (2016) 1697–1708.
[34] Y.T. Ahn, F. Zhang, B.E. Logan, J. Power Sources 247 (2014) 655–659.
[35] M.A. Kiani, M.F. Mousavi, S. Ghasemi, J. Power Sources 195 (2010) 5794–5800.
[36] H. Liu, B.E. Logan, Environ. Sci. Technol. 38 (2004) 4040–4046.
[37] Y.J. Feng, Q. Yang, X. Wang, B.E. Logan, J. Power Sources 195 (2010) 1841–1844.
[38] J. Liu, Y.J. Feng, X. Wang, Q. Yang, X.X. Shi, Y.P. Qu, N.Q. Ren, J. Power Sources 198 (2012) 100–104.
[39] J. Liu, F. Zhang, W.H. He, X.Y. Zhang, Y.J. Feng, B.E. Logan, J. Power Sources 261 (2014) 278–284.
[40] J. Liu, G.M. Geise, X. Luo, H.J. Hou, F. Zhang, Y.J. Feng, M.A. Hickner, B.E. Logan, J. Power Sources 271 (2014) 437–443.
[41] S.E. Oh, B.E. Logan, J. Power Sources 167 (2007) 11–17.
[42] R.R. Sayess, P.E. Saikaly, M. El-Fadel, D. Li, L. Semerjian, Water Res. 47 (2013) 881–894.
[43] S. Ishii, K. Watanabe, S. Yabuki, B.E. Logan, Y. Sekiguchi, Appl. Environ. Microbiol. 74 (2008) 7348–7355.
[44] Q. Zhang, J. Nghiem, G.J. Silverberg, C.D. Vecitis, Appl. Environ. Microbiol. 81 (2015) 4744–4755.
[45] H. Salehi, M. Rastgar, A. Shakeri, Appl. Surf. Sci. 413 (2017) 99–108.
[46] G. Zhao, Z. Schwartz, M. Wieland, F. Rupp, J. Geis-Gerstorfer, D.L. Cochran, B.D. Boyan, J. Biomed. Mater. Res. 74A (2005) 49–58.
[47] Y.S. Ye, M.Y. Cheng, X.L. Xie, J. Rick, Y.J. Huang, F.C. Chang, B.J. Hwang, J. Power Sources 239 (2013) 424–432.
[48] M. Soheilmoghaddam, H. Adelnia, H.C. Bidsorkhi, G. Sharifzadeh, M.U. Wahit, N.I. Akos, A.A. Yussuf, Macromol. Mater. Eng. 302 (2017) 1600260.
[49] S. Cheng, H. Liu, B.E. Logan, Electrochem. Commun. 8 (2006) 489–494.
[50] L. Zhuang, Y. Yuan, G.Q. Yang, S.G. Zhou, Electrochem. Commun. 21 (2012) 69–72.
[51] Q. Wen, S.Y. Wang, J. Yan, L.J. Cong, Z.C. Pan, Y.M. Ren, Z.J. Fan, J. Power Sources 216 (2012) 187–191.
[52] X.C. Cao, J. Ma, X.H. Shi, Z.J. Ren, Appl. Surf. Sci. 253 (2006) 2003–2010.
[53] M. Safarpour, A. Khataee, V. Vatanpour, Ind. Eng. Chem. Res. 53 (2014) 13370–13382.